Thermochemistry, Morphology, and Optical Characterization of Germanium Allotropes

Julia V. Zaikina, Elayaraja Muthuswamy, Kristina I. Lilova, Zachary Gibbs, Michael Zeilinger, G. Jeffrey Snyder, Thomas F. Fässler, Alexandra Navrotsky[*] and Susan M. Kauzlarich[*]

Supporting Information

X-ray powder diffraction and preferential orientation.

The initial XRD powder pattern of the synthesized *m-allo*-Ge differed drastically from the simulated one. While the XRD pattern can be indexed with the previously determined parameters [S1] (orthorhombic cell, a = 7.800(1) Å, b = 16.267(6) Å, c = 11.910(1) Å), the observed intensities of the peaks are considerably different (Figure S1 and S2). The reflections in the [00*l*] zone, *e.g.* 002, 004, 006 have enhanced intensities compared to the calculated ones. This indicates that the sample of *m-allo*-Ge suffers from preferential orientation, where the crystallites tend to orientate in the *ab*-plane. The diffraction pattern in this work was collected in reflection mode on a zero background flat holder, which favors the preferential orientation of the crystallites, while the reported powder pattern [S1] was obtained with capillary sample holder in transmission mode. Addition of X-ray amorphous SiO_2 to the sample results in a significant change of the intensities and reveals close resemblance to the reported powder pattern (Figure 3 in the text).

References:

[S1] Kiefer, F.; Karttunen, A. J.; Doblinger, M.; Fassler, T. F., Bulk Synthesis and Structure of a Microcrystalline Allotrope of Germanium (m-allo-Ge). *Chemistry of Materials* **2011,** 23, (20), 4578-4586.
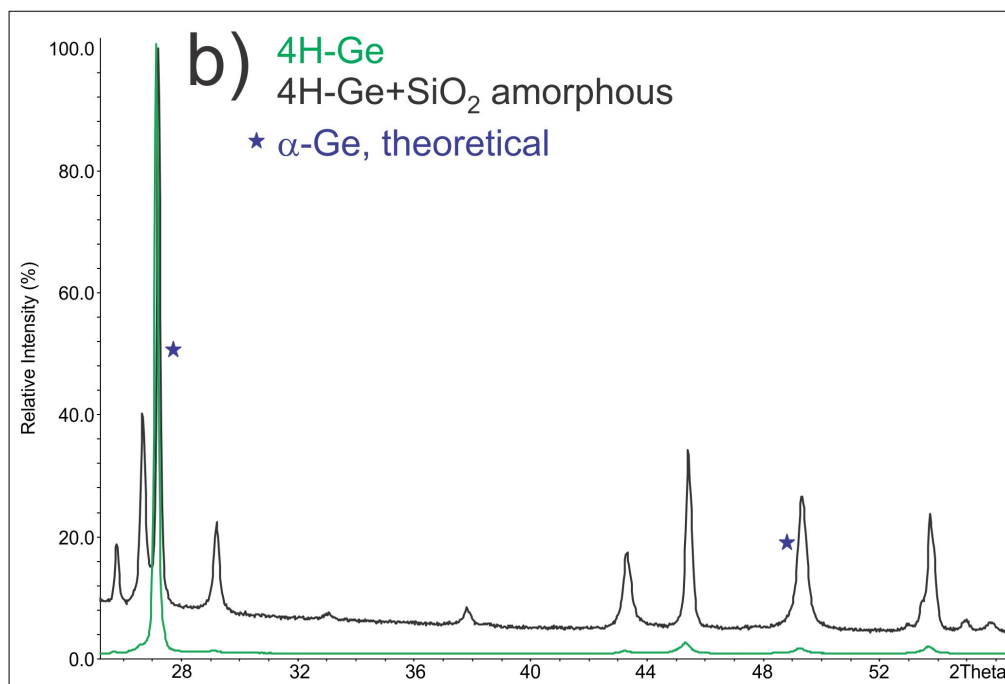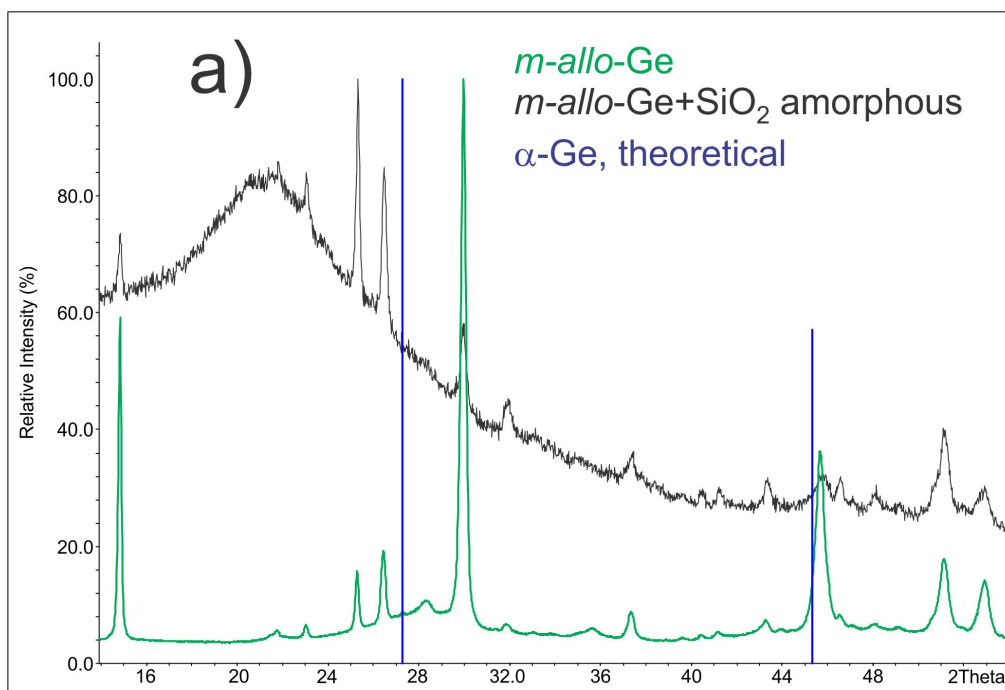
Figure S1. a) Powder X-ray diffraction patterns for allo-Ge sample with (black) and without (green) amorphous SiO₂ The theoretical pattern of the α-Ge impurity is shown in blue.

b) Powder X-ray diffraction patterns for 4H-Ge sample with (black) and without (green) amorphous SiO₂. The overlapping peaks of the α-Ge impurity are indicated with blue stars.
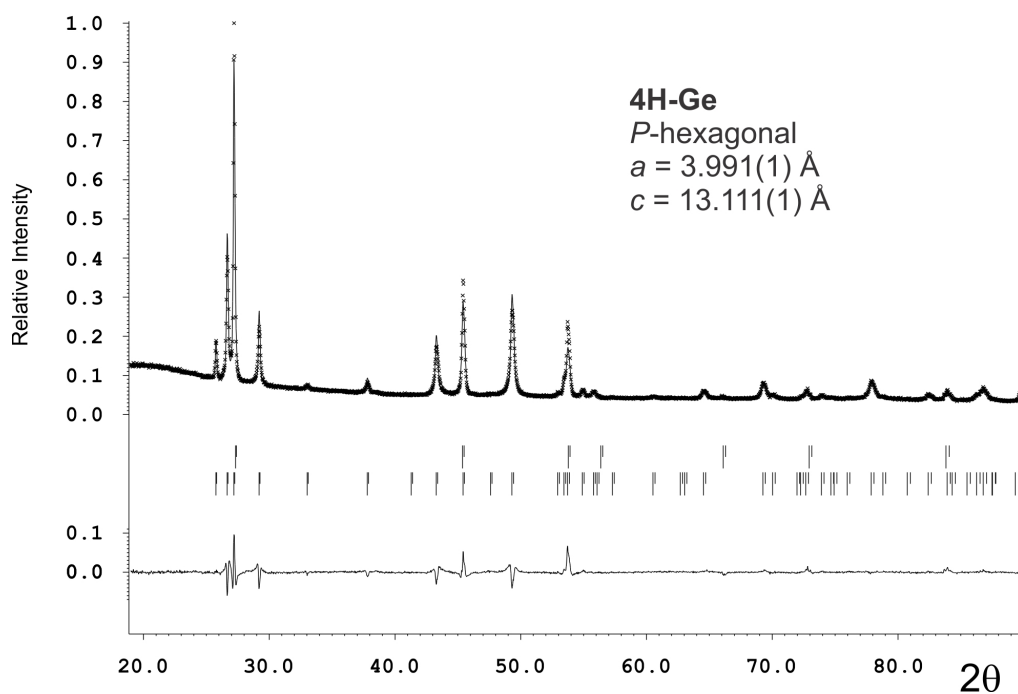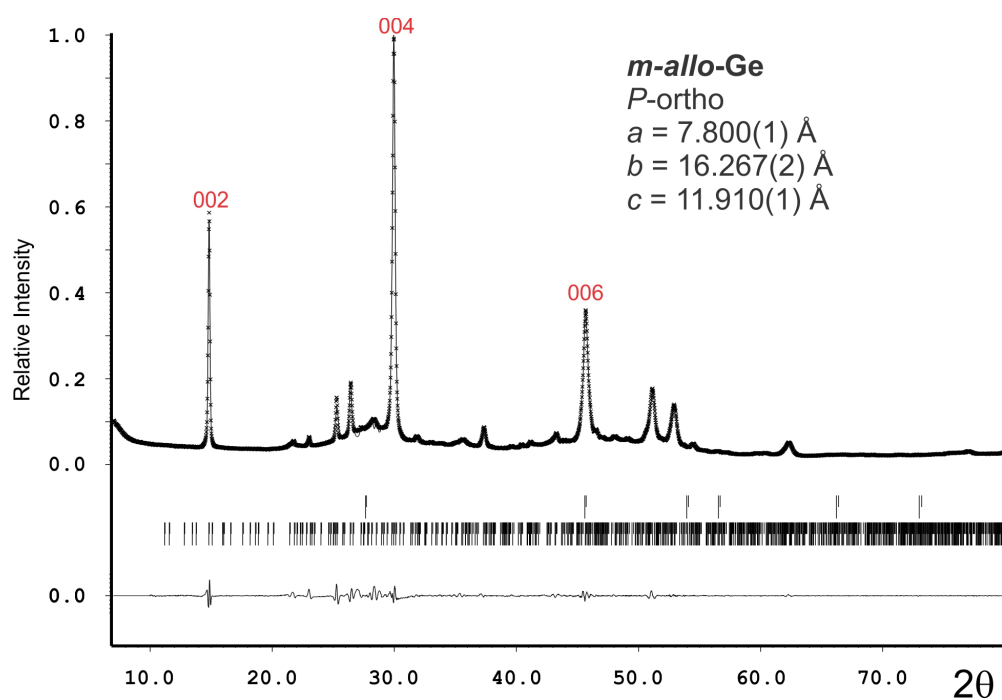
Figure S2. (top) Full-pattern profile fitting for the *m-allo*-Ge sample (Jana2000 program package). The *hkl* indexes of the reflections with enhanced intensity are indicated in red. Impurity of α-Ge is included into refinement.

(bottom) Powder X-ray diffraction patterns for 4H-Ge sample with SiO_2 amorphous. Impurity of α-Ge is included into refinement.
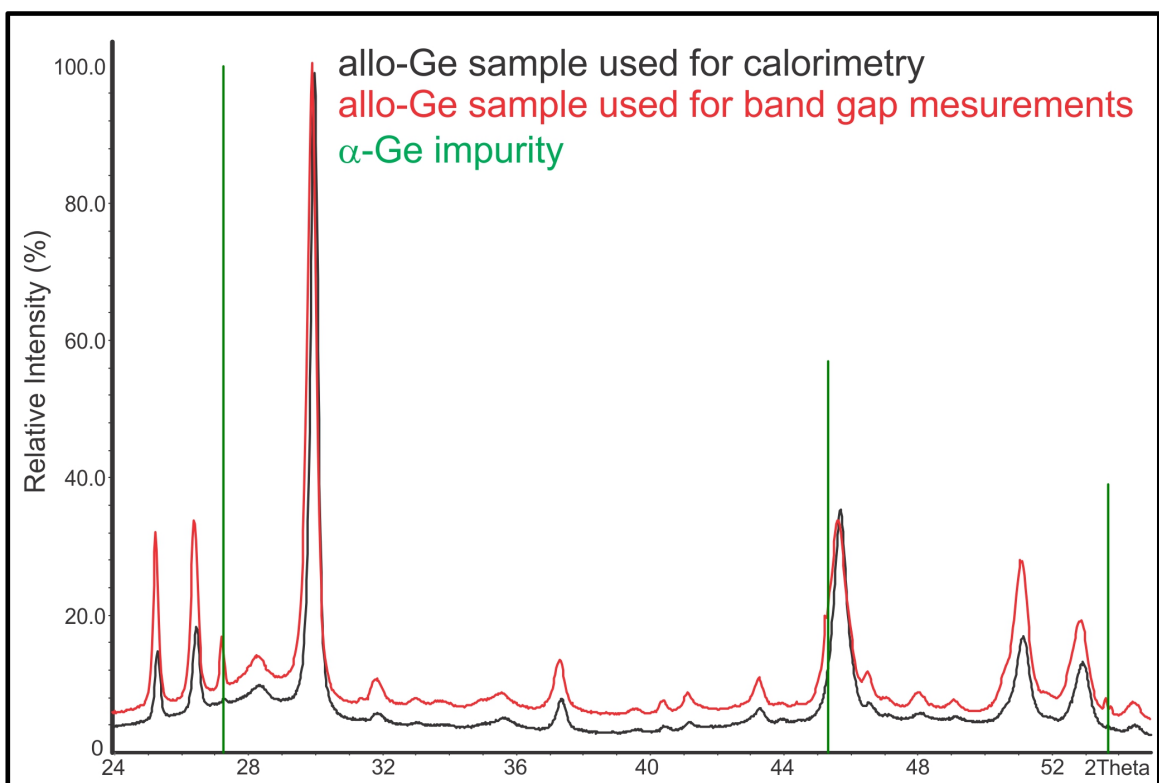
Figure S3. Powder X-ray diffraction patterns for *m-allo*-Ge samples with different amount of α-Ge impurity.
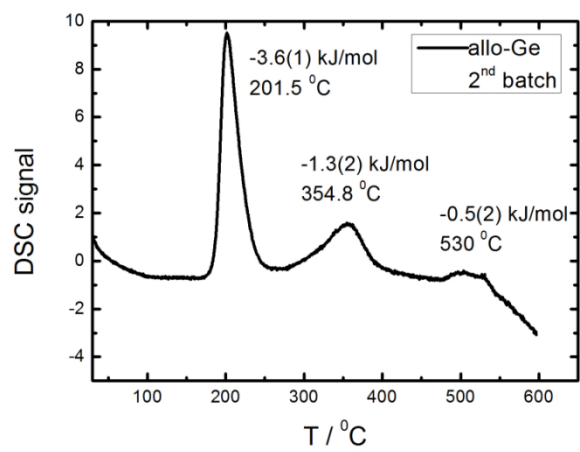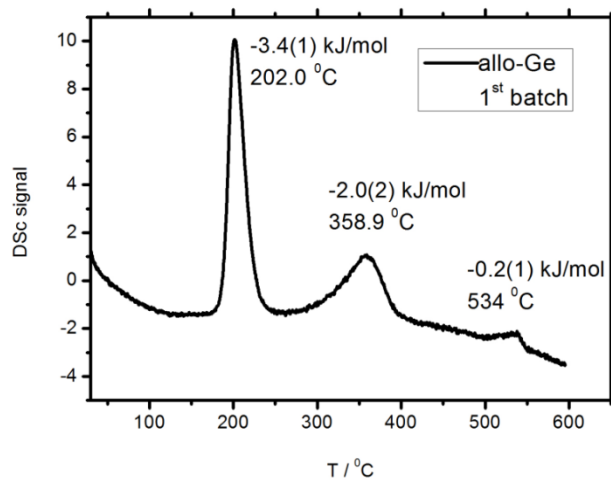
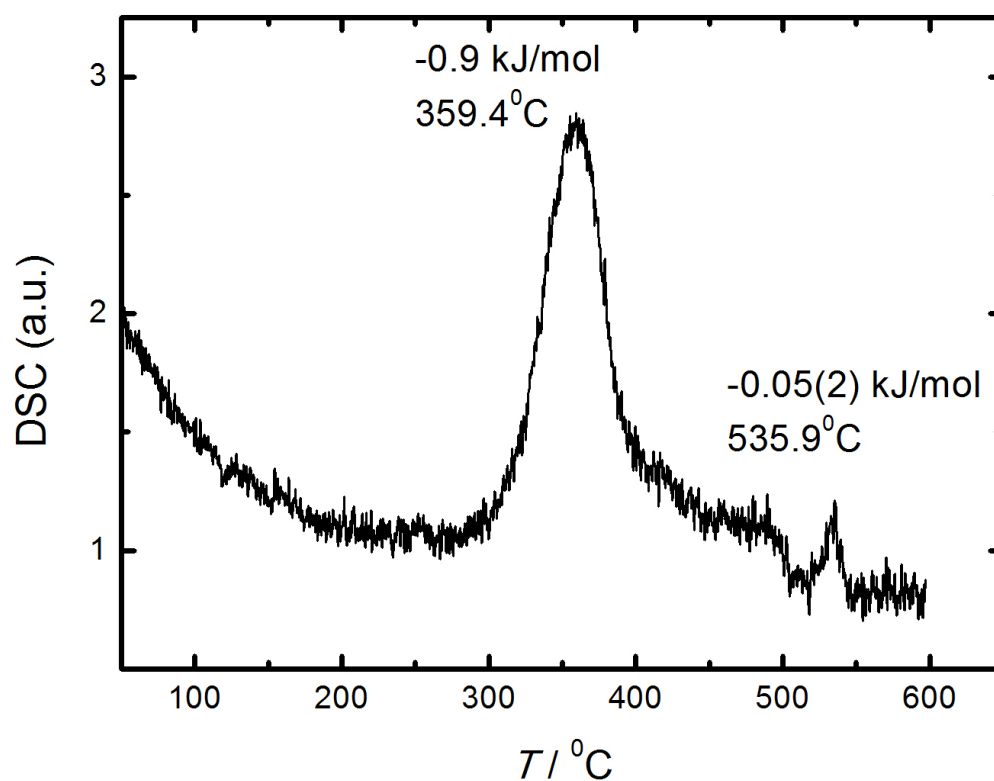**Figure S4**. DSC curves on heating of two samples of allo-Ge. No effects have been observed on cooling.

Figure S5. DSC curves on heating, showing transformation of 4H-Ge into α-Ge at 359°C with no significant mass change (weight gain < 0.9 wt.%). No effects have been observed on cooling.
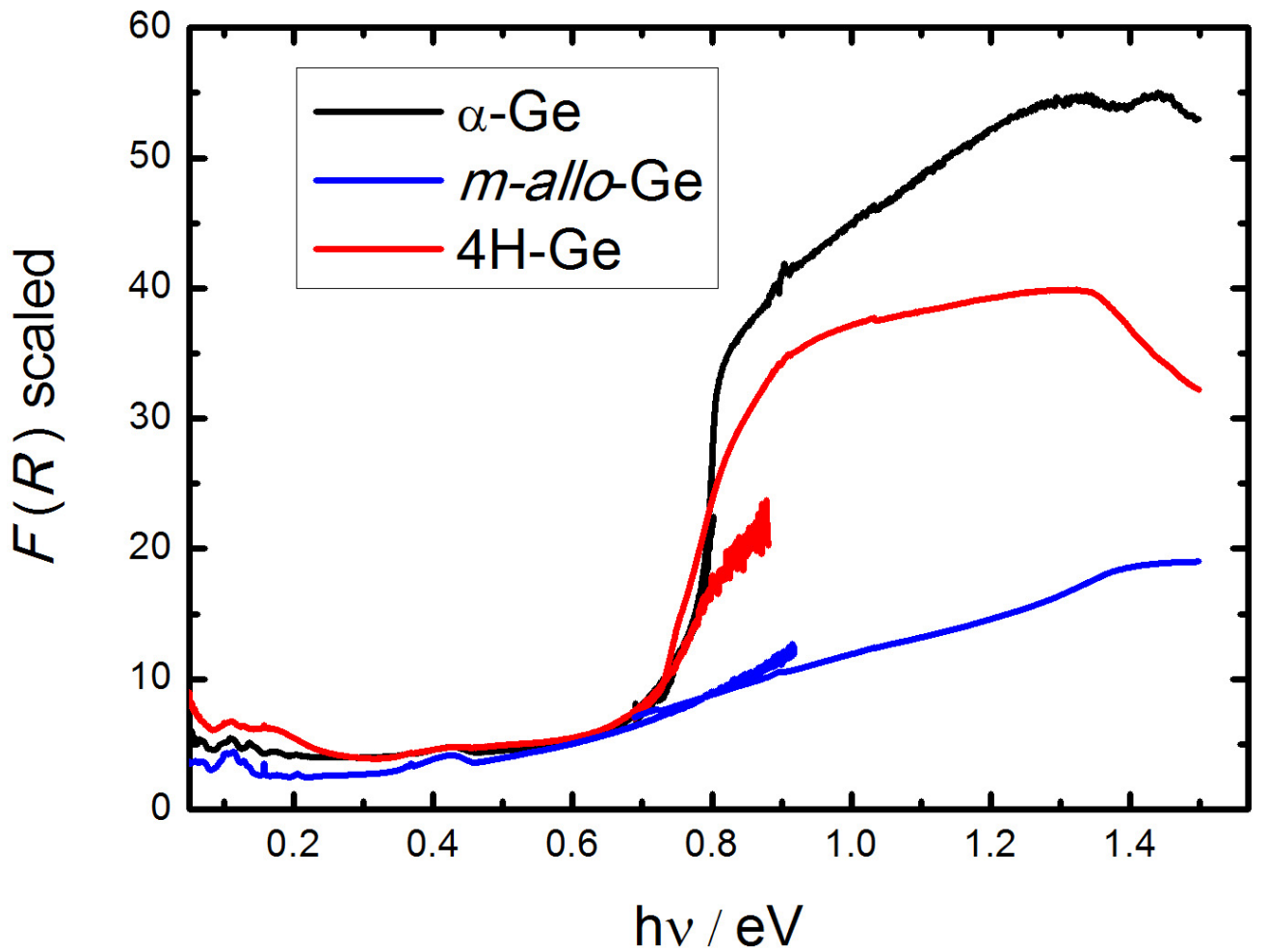
Figure S6. Optical absorption spectra of α-Ge (black), *m-allo*-Ge (blue) and 4H-Ge (red).

Figure S6 shows the Kubelka Munk function ($F(R)$=$(1-R)^2/2R = \alpha/S$) from the mid IR into the visible, where R is the fraction of light reflected, α is the absorption coefficient and S is the scattering coefficient. Features at around 0.2 eV could be due to the phonon modes in the germanium, and the broad bump at 0.4 eV was assigned to O-H stretching modes. Absorption edge measurements show an increasing Kubelka Munk function for energies above ~0.3 eV for all three Ge allotropes. It is not clear whether this is in fact inter-band absorption because it is obscured by O-H features around 0.4 eV. One could possibly vary the temperature to determine whether the feature might be associated with absorption or emission of phonons as in an indirect gap, but this was not done in this work.
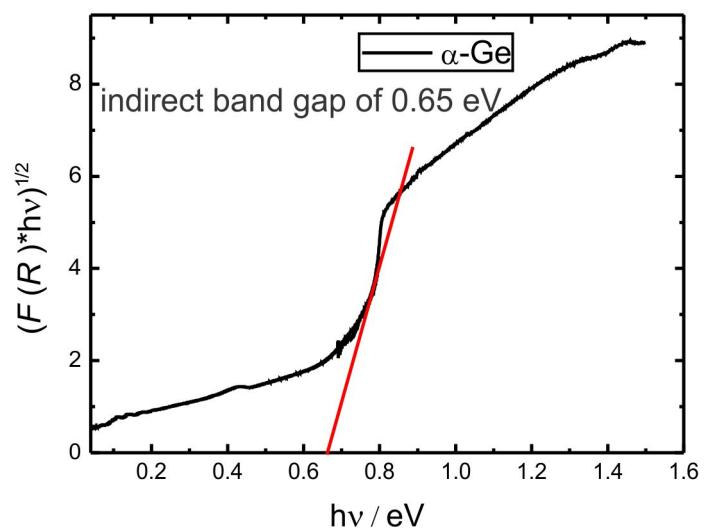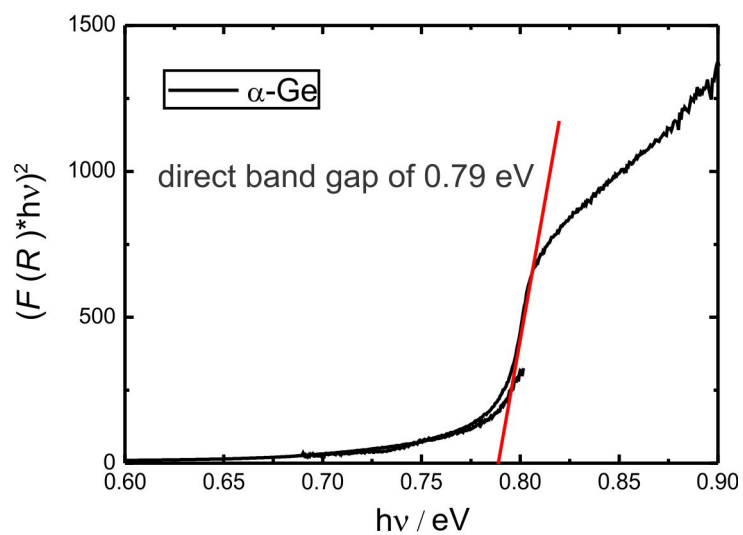
Figure S7. Tauc plot, $(F(R)*h\nu)^2$ *vs h*ν (top) and $(F(R)*h\nu)^{1/2}$ *vs h*ν (bottom) for α-Ge reference used for extrapolating direct and indirect band gaps (red line).